

A Liquid Xenon Detector for Positron Emission Tomography

M.I. Lopes, V. Yu Chepel, V. Solovov, R. Ferreira Marques and A.J.P.L. Policarpo

LIP-Coimbra, Department of Physics
University of Coimbra 3000 Coimbra
Portugal

Abstract

Here, we report on the present state of development of a liquid xenon detector composed by multiwire ionisation chambers, which has been developed for positron emission tomography (PET). It uses the fast scintillation signal for coincidence and subsequent trigger of the event processing. The charge signals induced on the wires are used for position determination along the radial and transaxial directions of the tomograph, as well as for energy information.

The following detector characteristics have been achieved: i) coincidence time resolution better than 1.5 ns (fwhm); ii) position precision along the radial direction equal to 5 mm; iii) position resolution in the transaxial direction of 0.8 mm (fwhm); iv) energy resolution of 17% (fwhm) for 511 keV γ -rays; v) efficiency of trigger of about 100%; vi) overall efficiency of detection of 60%.

The prospects for the development of this detector in view of its application in PET are discussed.

Introduction

Positron emission tomography (PET) is a medical imaging technique in which the patient is injected (or inhales) a biologically active tracer labelled with a positron-emitting isotope. Following the radioisotope decay, the positron annihilates with a nearby electron emitting two nearly collinear 511 keV γ -rays that can exit the patient body and be detected in the PET scanner. A positron annihilation is identified provided that the two photons are simultaneously detected. Thus, the radioisotope that gave rise to the emission is known to be located along the line defined by the two detected γ -rays. By accumulating many annihilation events, the spatial distribution of the radioisotope (and therefore the drug concentration) is reconstructed using the same methods as in computed tomography.

In almost all the clinical PET scanners, identical γ -rays detector modules are packed, as close as possible, forming concentric rings whose dimensions depend on the main clinical application of the tomograph. Each individual detector module must exhibit: high efficiency for 511 keV γ -rays, spatial resolution of the order of a few millimetres along two directions (corresponding to the axial and transaxial directions of the scanner), good time

resolution, low dead time, good energy resolution and low price (for a detailed discussion of the relative importance of these benchmarks and the desirable values for each of them, see [1]). Presently, the majority of commercial PET systems use as detector modules blocks of BGO (bismuth germanate, $\text{Bi}_4\text{Ge}_3\text{O}_{12}$) crystals coupled to two or four photomultipliers [2,3].

The main limitation of the present technology arises from the absence of information on the depth of interaction (DOI) of the photons in the crystals. In fact, the ring geometry of PET scanners results in many off-centre annihilation photons that enter the crystals at an angle other than the ideal normal incidence, penetrating into adjacent crystals and being consequently mispositioned [4]. This parallax (or elongation) artefact results in a progressive degradation of the spatial resolution from the centre towards the edge of the field-of-view of the scanner ring. Presently, this problem is addressed in commercial systems by oversizing the ring diameter so that there is an enough large central area where the DOI effect is minimal and thus the spatial resolution is fairly uniform. However, the price of the system can be substantially reduced and their performance improved if the PET scanner detectors give DOI information. In fact, spatial resolution and efficiency can be enhanced by making the detector modules, respectively, thinner (along the transaxial and axial directions) and longer. However, this would worsen the parallax effect and no net profit results. On the contrary, if the depth of interaction of the γ -ray within the detector module can be measured, the parallax can be corrected and the spatial resolution should be uniform throughout the entire field of view the scanner ring even for very thin and long detector modules.

Several ideas have been proposed to provide the PET detectors with DOI information but none of them has yet been applied to practical systems. Some of the most recent DOI encoding schemes proposed for crystals modules consists of: using detectors made of several scintillators with different decay times [5-7], coupling both transverse faces of the crystals to photosensitive detectors [8], using successive layers of scintillators slabs and wavelength shifter fibers [9], exploiting the difference of index of refraction between longitudinally adjacent scintillator segments and the compound optically coupling them [10].

The Liquid Xenon PET Module

Taking into account the above mentioned trend in PET scanners, we proposed a liquid xenon multiwire drift chamber as a detector module for PET [11,12] that has DOI sensitivity and can attain a performance in other benchmarks similar to that of the currently used BGO blocks.

It makes use of both the good properties of liquid xenon as a scintillator and the conduction of the free electrons produced by ionisation in the liquid. For a review of the properties of liquid xenon as detector medium, as well as its application to some specific detectors, see [13,14].

The proposed liquid xenon PET module is depicted schematically in Fig.1. It is composed by three cells, each 1 cm wide (x, the transaxial direction), 5 cm in depth (z, the radial direction) and 6 cm in length (y, the axial direction), separated by stainless steel planes (0.5 mm thick) that work as cathodes. The anode plane existing in the middle of each cell is formed by twenty wires ($\phi=50 \mu\text{m}$) stretched along the y-direction with a pitch of 2.5 mm and connected into pairs.

Charge signals induced on the wires are read individually. When a 511 γ -ray interacts in the liquid xenon, the depth of interaction is given directly by the position along z of the wire that exhibits signal. The transaxial coordinate of the interaction is obtained by measuring the drift time of the ionisation electrons, i.e., the rise time of the electronic component of the signal.

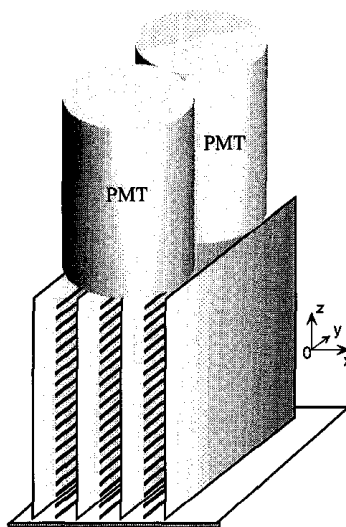


Fig.1 Scheme of the liquid xenon detector module for PET.

The scintillation light from liquid xenon is detected by two photomultipliers. The fast signal taken from their last dynode is used for coincidence and as the trigger for event processing, namely for starting the electrons drift time measurement.

We built a chamber composed by two modules similar to that depicted in Fig.1, mounted inside a stainless steel vacuum tight vessel equipped with

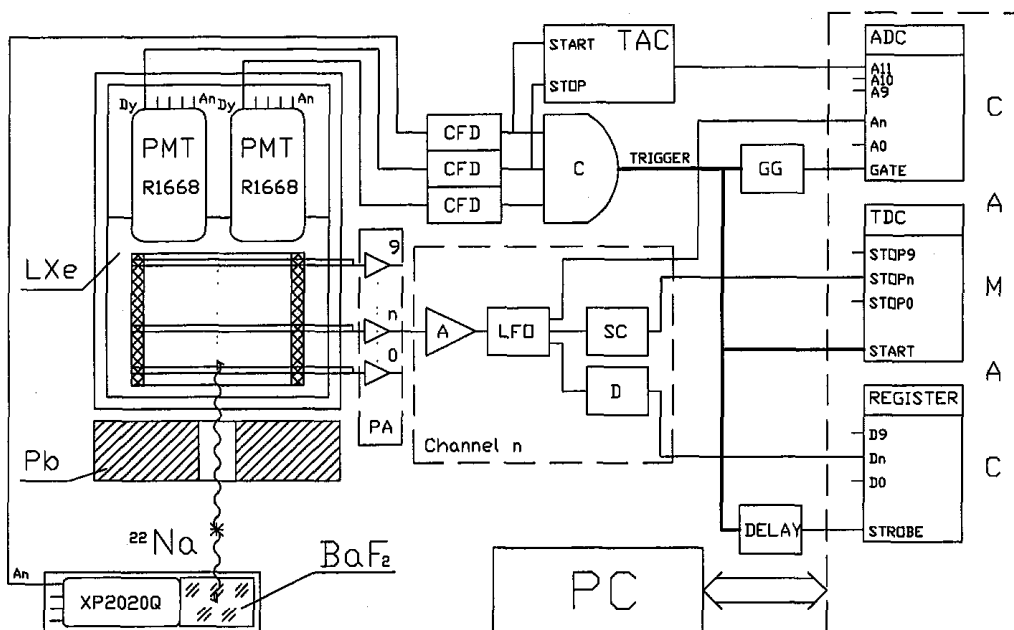


Fig.2 Readout and acquisition system for the liquid xenon cell: PMT: photomultiplier (An and Dy are its anode and dynode outputs, respectively); PA: charge preamplifier; A: linear amplifier; As: shaping amplifier; CFD: constant fraction discriminator; C: coincidence unit; LFO: linear FAN-OUT; SC: Stop-circuit; D: discriminator; GG: gate generator; TAC: time-to-amplitude converter; ADC: analogue to digital converter; TDC: time to digital converter; PC: IBM-type personal computer.

feedthroughs for high voltage and signals (a more detailed description is done elsewhere [12]). On the bottom, there is a stainless steel window. In the present design it is 1 mm thick but it can be made significantly thinner ($\approx 100 \mu\text{m}$ or less) to minimise the attenuation of the 511 keV γ -rays entering the detector.

The measurements reported here were carried out using only the central cell of one of the modules.

Experimental Set-up

Two Hamamatsu R1668 photomultipliers (PMTs), with 30 mm quartz windows, are installed inside the chamber such that their windows are immersed in liquid xenon.

The cathode planes are at -1000V while the anodes are at ground potential. Charge signals are read individually from each pair of wires and fed into low noise charge sensitive preamplifiers connected directly to the chamber feedthroughs and followed by amplifiers where no shaping is performed except a small integration of $0.1 \mu\text{s}$ for noise filtering. Preamplifiers [15] have r.m.s. noise of 400 electrons, rise time of 300 ns, decay time of $17 \mu\text{s}$ and operate at liquid xenon temperature.

The positron source is ^{22}Na mounted on a nickel plate for positron annihilation. To assure that mainly the central cell is irradiated, a 3 cm thick lead collimator with a hole of $8 \times 8 \text{ mm}^2$ was placed 2.3 cm below the chamber bottom and 8.3 cm above the source, the hole being aligned with the active cell (Fig.2).

To select the 511 keV γ -rays, the PMTs from the chamber are put in coincidence with a BaF_2 crystal ($\phi=50\text{mm}$ and 50 mm length), coupled to a Philips XP2020Q photomultiplier, placed under the cryostat and aligned with the collimator (see Fig.2)

The chamber, the collimator and the source are mounted on a rigid frame and placed inside a cryostat cooled by liquid nitrogen. An adjustable electrical heater wound around the chamber allows operating the chamber at the desired temperature [16]. The data reported here were taken at a temperature between -95°C and -105°C varying from run to run but with stability during each run of $\pm 2^\circ\text{C}$.

The xenon is purified by several passages of the gas through an Oxisorb column. The electron lifetime was measured to be $> 20 \mu\text{m}$, this limit being set by the sensitivity of the impurity monitor method [17].

The electronic and data acquisition system is schematically depicted in Fig.2 and it is described in detailed in [18].

Detector Evaluation: Experimental results

Time resolution

For the measurement of the time spread of the $2\text{-}\gamma$ coincidences, the threshold of the CFD connected to the BaF_2 PMT was set at 100 keV and those of the CFDs connected to the chamber PMTs were varied between 1 and 10 photoelectrons.

The time distribution of coincidence events without applied electric field is shown in Fig.3. The measured value for the time resolution of the chamber- BaF_2 is 1.3 ns (fwhm). The same resolution is obtained when high voltage is applied to the cathodes.

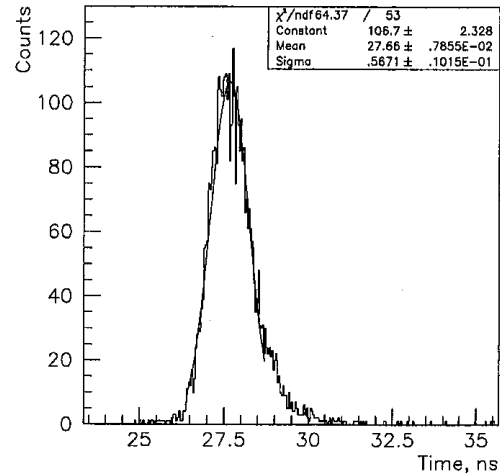


Fig.3 Time resolution of the liquid xenon cell- BaF_2 system.

Depth of Interaction Sensitivity

When electrons produced by the γ -ray interaction drift towards the anode plane, charge is induced in both the collecting pair of wires and the nearest adjacent one. For a better depth of interaction sensitivity it is necessary to identify unambiguously the collecting pair of wires.

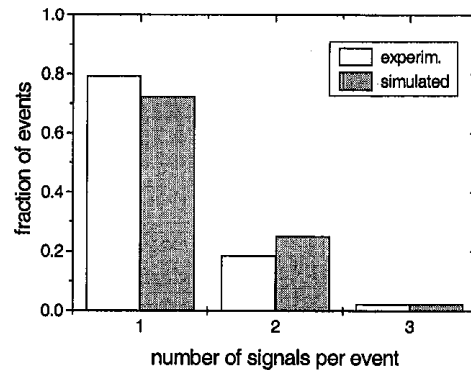


Fig.4 Distribution of the number of charge signals per event: experimental (white) and calculated by simulation (grey)

Computations of the pulse shape of the charge signals induced on the wires have shown that the signal in the collecting pair and in the neighbour have very different shapes [19], fact that was confirmed experimentally [18]. Hence, the identification of the collecting pair and the rejection of the signal induced

on its neighbours is achieved by pulse shape discrimination, as discussed elsewhere [18].

The reliability of the rejection method and the depth of interaction sensitivity can be assessed by comparing the distribution of the number of signals per event recorded experimentally with that predicted by simulation. This comparison is made in Fig.4 for signals above a threshold set equal to 2000 electrons. The absence of an increase in the number of the events with two signals relatively to that predicted by the simulation, shows that the rejection method is effective. Thus, the depth of interaction is simply given by the pitch of pairs of wires in the cell, presently equal to 5 mm.

Energy Resolution

The energy resolution of an ionisation chamber without Frisch grid, is very poor due to the positive ions effect. The pulse height distribution of the charge signal read on a wire of the liquid xenon cell

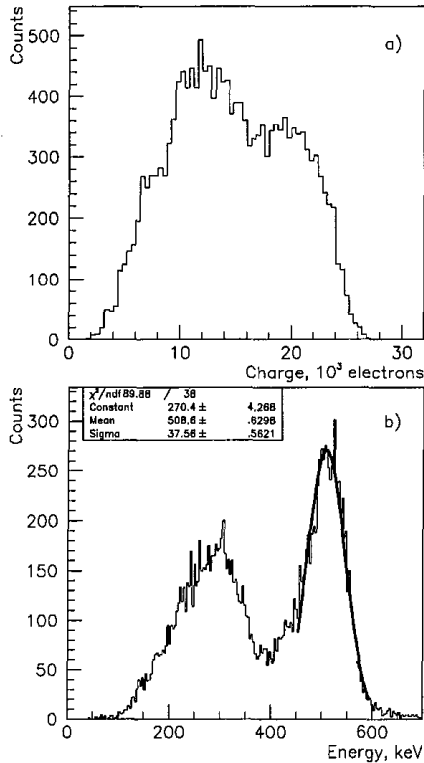


Fig.5 Amplitude spectrum of charge signals on a wire without correction (a) and after correction (b).

is shown in Fig.5a. However, the energy resolution can be substantially improved by exploiting the correlation between the induced charge on the wire and the electron drift time [18]. Once the drift time is measured, this correlation allows correcting the pulse height from its dependence on the interaction point position in the cell. The corrected spectrum is shown in Fig.5b. A gaussian fit gives an energy resolution of 17.2 ± 0.2 % FWHM.

Transaxial Position Resolution

To assess the position resolution of the detector along the x-direction (transaxial direction in the tomograph) for 511 keV γ -rays, the distribution of the electrons drift time was recorded. The resolution can be determined by fitting the distribution of Fig.6. The best fit gives $\sigma_t = 0.16 \pm 0.01$ μ s. Hence, the transaxial position resolution is 0.8 ± 0.05 mm (fwhm), taking the electron drift velocity 2 mm/ μ s at 2 kV/cm [20]. This value for the position resolution is in good agreement with a previous estimate made on the basis of measurements carried out with α -particles emitted by a source deposited on the cathode [21].

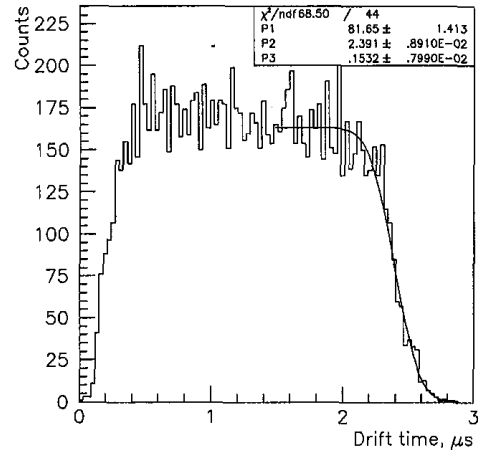


Fig.6 Drift time spectrum.

Efficiency

The overall efficiency of detection for 511 keV γ -ray in the liquid xenon cell is given by the product of three factors: the interaction probability of the photon in the liquid filling the active volume of the cell (P_i), the probability that the scintillation light produced is detected and triggers the event acquisition (P_d) and the probability that, in the case of the event being triggered, the electrons released in the interaction produce on the wires at least one charge signal above threshold (P_q).

P_i was analytically calculated to be 73% for 511 keV γ -rays, taking for the density of the liquid 2.9 g/cm³ and for the attenuation coefficient 0.0898 cm²/g. P_d was estimated from the behaviour of the signal count distribution along the z-direction for different charge discrimination thresholds [17]. From the fact that the shape of this distribution was constant for discrimination levels above ≈ 50 keV, one can conclude that P_d is about 100%. Finally P_q was measured as the fraction of triggered events, involving the interaction of a 511 keV γ -ray in the active volume of the cell, for which at least one charge signal is recorded. For energy depositions above 50 keV, P_q is about 80%.

Thus, the overall detection efficiency for 511 keV γ -rays is about 60%.

Axial Position Resolution

With the present design, the information on the axial coordinate of the interaction point in the detector is obtained from the light sharing between the two PMTs using an Anger type logic. Preliminary calculations show that the position resolution strongly depends on both the depth of interaction and the axial coordinate. In the central plane of the cell perpendicular to the wires, it varies between 20 mm and 1 mm, improving with the proximity of the interaction point to the PMTs but it gets much worse at the borders of the cell.

Conclusion

The performance of the liquid xenon module is very promising as far as depth of interaction sensitivity, time resolution, axial position resolution and energy resolution are concerned. The efficiency is lower than with BGO crystals but it can be improved by increasing the depth of the cells.

Considering the present requests for PET systems, the axial resolution is not good enough. A possible alternative is to replace the Anger logic by an algorithm of maximal likelihood applied to the amplitude of the PMTs signals. Methods based on the charge signal are also being considered. One of them consists in replacing the anode wires by a plane of strips with two-dimensional readout.

References

- [1] W.W. Moses, S.E. Derenzo, T.F. Budinger, "PET detector modules based on novel detector technologies", *Nucl. Instr. and Meth.*, A353, pp.189-194, 1994.
- [2] M.E. Casey and R. Nutt, "A multocrystal two dimensional BGO detector system for positron emission tomography", *IEEE Trans. Nucl. Sci.*, Vol.NS-37, pp.460-463, 1986.
- [3] M.P. Tornai, G. Germano and E.J. Hoffman, "Positioning and Energy Response of PET Block Detectors with Different Light Sharing Schemes", *IEEE Trans. Nucl. Sci.*, Vol. 41, no. 4, pp.1458-1463, 1994.
- [4] E.J. Hoffman, T.M. Guerrero, G. Germano, W.M. Digby and M. Dahlbom, "PET system calibrations and corrections for quantitative and spatially accurate images", *IEEE Trans. Nucl. Sci.*, Vol.36, pp. 1108-1112, 1989.
- [5] Wai-Hoi Wong, "A positron camera design with cross-coupled scintillators and quadrant sharing photomultipliers" *IEEE Trans. Nucl. Sci.*, Vol.40, pp. 962-966, 1993.
- [6] S. Yamamoto and H. Ishibashi, "A GSO depth of interaction detector for PET", *IEEE Trans. Nucl. Sci.*, Vol.45, pp. 1078-1082, 1998.
- [7] M. Schmand, L. Eriksson, M.E. Casey, M.S. Andreaco, C.Melcher, K.Wienhard, G.Flügge, R. Nutt, "Performance results of a new DOI detector block for a high resolution PET-LSO research tomograph HRRT", *1997 IEEE NSS/MIC Conf. Record*, CD-ROM, paper M02_02.
- [8] W.W. Moses, S.E. Derenzo, C.L. Melcher and R.A. Manente, "A room temperature LSO/PIN photodiode PET detector module that measures depth of interaction", *IEEE Trans. Nucl. Sci.*, Vol.42, pp.1085-1089, 1998.
- [9] W. Worstell, O. Johnson and V. Zawarzin, "Development of high resolution PET detector using LSO and wavelength-shifting fibers", *Conf. Record of 1995 IEEE MIC*, Vol.3, pp. 1756-1760, 1995.
- [10] C. Moisan, M.S. Andreaco, J.G. Rogers, S. Paquet and D. Voza, "Segmented LSO Crystals for depth of interaction encoding in PET", *1997 IEEE NSS/MIC Conf. Record*, CD-ROM, paper M06_25.
- [11] V.Yu. Chepel, "A New Liquid Xenon Scintillation Detector for Positron Emission Tomography", *Nucl.Tracks Rad. Meas.*, Vol.21, pp. 47-51, 1993.
- [12] V.Yu. Chepel, M.I. Lopes, H.M. Araújo, M.A. Alves, R.F. Marques and A.J.P. Policarpo, "Liquid Xenon Multiwire Chamber for Positron Tomography", *Nucl. Instr. and Meth.*, Vol.A367, pp.58-61, 1995.
- [13] T. Doke, "Fundamental properties of liquid argon, krypton, and xenon as radiation detector media", *Portug. Phys.*, 12, pp.1-48, 1981.
- [14] T. Doke and K. Masuda, "Present status of liquid rare gas scintillation detectors and their new application to gamma-ray calorimeters", *Nucl. Instr. and Meth.*, A420, pp.62-80, 1999.
- [15] TOTEM 2.2, developed by the ICARUS group at CERN; P. Benetti, A. Bettini, E. Calligaris et al., "A Three-ton Liquid Argon Time Projection Chamber", *Nucl. Instr. and Meth.*, Vol.A332, pp.395-412, 1993.
- [16] V.Y. Chepel, M.I. Lopes, R. Ferreira Marques and A.J.P.L. Policarpo, "Purification of Liquid Xenon and Impurity Monitoring for a PET Detector", *Nucl. Instr. and Meth.*, A349, pp.500-505, 1994.
- [17] V. Yu Chepel, V. Solovov, J. van der Marel, M.I. Lopes, P. Crespo, Dinis Santos, R.F. Marques, A.J. Policarpo, "The liquid xenon detector for PET: recent results", presented at 1998 *IEEE Nucl. Sci. Symp. Med. and Imag. Conf.*
- [18] P. Crespo, J. van der Marel, V. Yu Chepel, M.I. Lopes, Dinis Santos, R.F. Marques, A.J. Policarpo, "Pulse Processing for the PET liquid xenon multiwire chamber", presented at 1998 *IEEE Nucl. Sci. Symp. and Med. Imag. Conf.*,
- [19] P. Crespo, V. Chepel, M.I. Lopes, L. Janeiro, R.F. Marques and A.J. Policarpo. "Pulse Shape Analysis in the Liquid Xenon Multiwire Ionisation Chamber for PET", *IEEE Trans. Nucl. Sci.*, Vol.45, pp.561-567, 1998.
- [20] L.S. Miller, S. Howe and W.E. Spear, "Charge Transport in Solid and Liquid Ar, Kr and Xe", *Phys. Rev.*, Vol. 166, no 3, pp.871-878, 1968.
- [21] V.Yu. Chepel, M.I. Lopes, A. Kuchenkov, R.F. Marques and A.J. Policarpo, "Performance Study of Liquid Xenon Detector for PET", *Nucl. Instr. and Meth.*, Vol.A397, pp.427-432, 1997.